Numerical Simulation of Non-Equilibrium Plasma Discharge for High Speed Flow Control

Ramakrishnan Balasubramanian, Karupannasamy Anandhanarayanan, Rajah Krishnamurthy & Debasis Chakraborty

Journal of The Institution of Engineers (India): Series C
Mechanical, Production, Aerospace and Marine Engineering

ISSN 2250-0545

J. Inst. Eng. India Ser. C
DOI 10.1007/s40032-016-0314-1

Springer

Your article is protected by copyright and all rights are held exclusively by The Institution of Engineers (India). This e-offprint is for personal use only and shall not be self-archived in electronic repositories. If you wish to self-archive your article, please use the accepted manuscript version for posting on your own website. You may further deposit the accepted manuscript version in any repository, provided it is only made publicly available 12 months after official publication or later and provided acknowledgement is given to the original source of publication and a link is inserted to the published article on Springer's website. The link must be accompanied by the following text: "The final publication is available at link.springer.com".

Author's personal copy

J. Inst. Eng. India Ser. C
DOI 10.1007/s40032-016-0314-1

ORIGINAL CONTRIBUTION

Numerical Simulation of Non-Equilibrium Plasma Discharge for High Speed Flow Control

Ramakrishnan Balasubramanian[1] · Karupannasamy Anandhanarayanan[1] · Rajah Krishnamurthy[1] · Debasis Chakraborty[1]

Received: 24 February 2015 / Accepted: 23 May 2016
© The Institution of Engineers (India) 2016

Abstract Numerical simulation of hypersonic flow control using plasma discharge technique is carried out using an in-house developed code CERANS-TCNEQ. The study is aimed at demonstrating a proof of concept futuristic aerodynamic flow control device. The Kashiwa Hypersonic and High Temperature wind tunnel study of plasma discharge over a flat plate had been considered for numerical investigation. The 7-species, 18-reaction thermo-chemical non-equilibrium, two-temperature air-chemistry model due Park is used to model the weakly ionized flow. Plasma discharge is modeled as Joule heating source terms in both the translation-rotational and vibrational energy equations. Comparison of results for plasma discharge at Mach 7 over a flat plate with the reference data reveals that the present study is able to mimic the exact physics of complex flow such as formation of oblique shock wave ahead of the plasma discharge region with a resultant rise in surface pressure and vibrational temperature up to 7000 K demonstrating the use of non-equilibrium plasma discharge for flow control at hypersonic speeds.

Keywords Plasma discharge · Joule heating · Non-equilibrium flow · CERANS-TCNEQ

List of symbols

A	Area of surface
C_s, c_s	Mass fraction of species
D_s	Species mass diffusion coefficient
E	Specific energy
e_{ve}	Specific vibrational-electron electronic energy
$\mathrm{E_{ve}}$	Total vibrational-electron electronic energy
$\vec{F}_j$	Flux vector in the jth direction
$\mathrm{h_s}$	Total enthalpy of species
I_s	Mass diffusion species
$\mathrm{J_{i,j}}$	Mass diffusion of the jth species along the ith direction
M_s, $\mathcal{M}_s$	Molecular weight of the species
M	Mach number
ns, nr	Number of Species
$\hat{n}_j$	Component of surface outward normal
N_s	Number density of species
$\vec{q}_i$	Heat flux along ith direction
T	Time in seconds
T, $\mathrm{T_v}$	Translational-rotational, vibrational temperature
U	Conserved variable vector
U_n	Contra-variant velocity
V	Volume of cell element
u, v, w	Velocity components along x, y, z directions
x, y, z	Cartesian coordinate directions
Q	Net Joule heat added per unit length

Greek Symbols

δ_{ij}	Kronecker delta
κ	Thermal conductivity of the gas
μ	Coefficient of molecular viscosity of the gas
μ_s	Coefficient of molecular viscosity of species
ρ_i	Density of ith species
τ_{ij}	Viscous shear stress
$\vec{\omega}$	Source term
$\vec{\Omega}$	Source term vector

✉ Ramakrishnan Balasubramanian
bals.cfd@gmail.com; r_balasubramanian@drdl.drdo.in

[1] Defence Research and Development Laboratory, Kanchanbagh, Hyderabad 500058, India

Published online: 16 June 2016

Author's personal copy

Introduction

Aerodynamic control concepts of futuristic hypersonic flight vehicle such as AJAX [1] extensively depend only on usage of non-intrusive means of flow control in lieu of the protruding conventional controls having moving parts and surfaces which might be subjected to severe aerodynamic heating, thereby necessitating complex thermal protection systems. Recently, the use of electro-magnetic force control actuators which rely on techniques such as focused plasma discharge, electron beam ionization as well Magnetohydrodynamics are gaining wide attention for their potentially overweighing benefits over the conventional control surfaces [2]. In such proof of concept studies which have promising avenues in hypersonic flight vehicle actuation, it is necessary to build a robust and reliable technology base that can significantly contribute towards in-house research, design and development of these new challenging avenues.

Wind tunnel experiments involving hypersonic flow with plasma discharge for actuation studies are gaining prominence, whereas not many computational tools considering relevant mathematical models are available for numerically mimicking the problem. Towards this step, a numerical toolkit namely, CERANS-TCNEQ [3] had been developed for simulation of complex physics associated with hypersonic non-equilibrium flows, characterized for standard reentry flow applications and extended for the plasma discharge based flow control problem in a novel way. It is a 3D finite volume Navier–Stokes solver for simulating ionized flow using seven species finite-rate air-chemistry model involving a total energy conservation equation for energy partitions such as translational, rotational, vibrational and electronic energies. In addition an equation for conservation of vibrational energy is solved for modeling the vibrational excitation and dissociation of the molecular species. More details on the CERANS-TCNEQ code can be obtained from [3–5]. In the present work, the code is applied to demonstrate a novel proof-of-concept flow control technique using plasma discharge and the results are compared with standard literature.

Plasma Actuation Methods

Aerodynamic flow control for flight vehicles shall be broadly categorized into mechanical and energetic methods [6]. Typical examples of conventional mechanical methods of flow control are the vortex generators, boundary layer tripping devices and suction and blowing over wings and control surfaces for flow separation controls. These mechanical methods are highly suitable for flight vehicles flying in speed regimes up to high supersonic Mach numbers. However the disadvantages of using such devices are high drag penalty due external protrusion of the surfaces which are intrusive to the flow causing high flow distortion. They require housing of many moving parts, requires several separate actuation mechanisms. In case of high speed flows, especially in hypersonic flights, external protrusion of a surface for flow control results in it subjected to severe aerodynamic heating. Hence it is necessary to provide complex active or semi-active cooling of surfaces for thermal protection. Housing of several actuation mechanisms implies weight penalty of the overall flight vehicle. Also for the mechanical means of aerodynamic flow control, the actuation response time is limited to the characteristics of mechanical actuators.

On the contrary, energetic means of aerodynamic control are gaining world-wide attention due several advantages such as, non-intrusive to flow and flexibility without any moving parts, ease of arrangement/piloting of the flow control device set-up, high actuation frequency with pulsing mode of operation, effectiveness for wide range of flight conditions and can have multiple options of electromagnetic force control (EMFC) actuations. The energy sources for the energetic methods are direct current arc discharge mechanism, microwave, electrical beam, electric discharge and laser beam. For the AJAX [1] class of hypersonic scramjet based research vehicle, the EMFC based actuators considered includes, focused plasma discharge, electron beam ionization (laser deposition) and the above coupled with electromagnetic fields.

Shang et al. [7] carried out experimental and computational investigations of plasma actuation mechanism in hypersonic flows using glow discharge. Extensive experimental and numerical investigations are carried out by Watanabe and Suzuki [8] for studying impulsive plasma discharge in a Mach-7 hypersonic flow over a flat plate, a compression and an expansion corner [9]. They observed that the plasma discharge has enormous potential to modify the surface pressure distribution and can offer benefits such as lift enhancements as well as steering moments. Yang [6] studied flow control using laser energy deposition at Mach 5 using qualitative and quantitative measurement techniques and observed that surface pressure and heat transfer rate have been redistributed.

In order to investigate the flow control benefits of plasma actuation, the present study is aimed at demonstrating the capability of the CERANS-TCNEQ code by characterizing it for the test case presented in [8] that of plasma discharges over a flat plate in hypersonic flow. The effect of plasma discharge on the hypersonic flow field for modifying the surface pressure distribution had been modeled and simulated for realizing a possible flight vehicle actuation. Plasma discharge experiment conditions in the Kashiwa Hypersonic and High Temperature Wind

Author's personal copy

Tunnel [8, 9] of University of Tokyo are taken as test case for validation. The flow conditions of their experiment are Mach number 7, stagnation pressure 950 kPa, and the stagnation temperature varied from 570 to 610 K (static temperature is 54.63 K with flow density being 0.01463 kg/m^3). The DC plasma discharge over the flat plate had been realized using 500 V DC power supply at 6 Amperes. In their numerical simulations [8] they have used a 11 species thermo chemical non equilibrium solver with heat addition in the form of Joule heating sources to the translational and vibrational energy partitions.

CERANS-TCNEQ Code

CERANS [10] (Compressible Euler-Reynolds Averaged Navier–Stokes) is a three-dimensional finite volume RANS solver developed in-house for solving external aerodynamic flows past complex flight vehicle configurations [11]. In order to various complex physico-chemical processes occurring due to hypervelocity flow, it is necessary to consider air-chemistry with chemical and thermal non equilibrium effects in the mathematical model. Hence, the CERANS code had been modified to include non-ionizing thermo-chemical non-equilibrium model due to Park [12] for numerical simulation of complex flows and the code is henceforth called CERANS-TCNEQ [4, 5] (CERANS Thermo-Chemical Non-Equilibrium). This code had been validated for hypersonic flow problems involving real gas effects.

The non-ionizing flow simulation solver uses the two temperature, five-species (N_2,O_2,NO,N and O), 17 reaction thermo-chemical non-equilibrium model along with the AUSM-PW + numerical flux function for modeling the convective terms and central differencing approximation for the viscous terms. The energy relaxation occurring due to the dissociation of molecular species had been handled separately by a conservation equation for vibrational energy resulting in the evaluation of the vibrational temperature of the gas mixture. Overall, the non-ionizing CERANS-TCNEQ code solve for five species mass conservation equations, one total mass conservation equation, three momentum conservation equations, one vibrational energy conservation equation, one total energy conservation equation.

The physical process of ionization of gas species becomes predominant in case of reentry of flight vehicles or plasma discharge as considered in the present work. In order to solve hypersonic flow problems which involve the process of ionization, in addition to dissociation and recombination of species, it is necessary to consider the additional complexities arising due to ionization in the existing computation model. Towards this, the CERANS-TCNEQ code had been extended [5] for solving the additional ionizing species namely NO^+ and e^-, respectively the ionic nitric oxide and the electron. So, the ionizing CERANS-TCNEQ code solves, 7 species, 18-reaction, thermo-chemical non-equilibrium model. It is assumed that the electronic temperature, which defines the electronic excitation state of the gas, is in equilibrium with the vibrational temperature, thereby avoiding the complexity of introducing an additional equation for the conservation of electronic energy. The code had been validated [5] for standard ionizing hypersonic reentry flow test cases with very good comparison with literature. In this work, this code had been further extended for addressing the plasma discharge through joule heating involving weak ionization. The details are presented in next section.

In CERANS-TCNEQ, the higher order spatial accuracy for the flow field variables is obtained using the method of reconstruction. The interfacial flow gradients required for the evaluation of viscous stresses are obtained by using cell-centered weighted least squares method for structured grids. The viscous flow gradients at the interface are further corrected for avoiding odd–even decoupling. Barth's min–max limiter had been used for preserving monotonicity.

The aim of the present study is to demonstrate the simulation capability and accuracy of CERANS-TCNEQ for aerodynamic actuation mechanism by plasma discharge as a proof of concept study for futuristic aerodynamic flow control.

Governing Equations for Modelling Plasma Discharge

The system of governing equations for ionizing air-chemistry consists of 7 species continuity equations. In general, the total energy is partitioned into translational, rotational, vibrational and electronic modes and hence requires representation of separate energy equation for each of these modes. Several approximations are made for reducing the complexity in description of various energy modes [13] and some that are considered in the present implementation is discussed.

In case of non-ionizing thermo-chemical non-equilibrium flow model, the partition energy due to vibrational mode is represented by a separate vibrational energy conservation equation and its evaluation leads to determination of the vibrational temperature T_v which describes the state of vibrational excitation of the mixture. Also the rotational energy mode is assumed equilibrated with the translational energy mode and hence can be evaluated from the total energy conservation equation. Such model which describes evaluation of two temperatures for representing translational-rotational and vibrational states is called the two-temperature model.

Author's personal copy

However, for modeling the ionization effects, the partition energy corresponding to the electronic mode needs to be defined. This requires a separate electron and electronic excitation energy conservation equation [13] and its evaluation leads to determination of the electronic temperature T_e which describes the electronic state of the mixture. Such a model which requires evaluation of three unique temperatures for describing all the partition modes is called a three-temperature model. An alternative possibility is to consider the two-temperature framework within which the essence of energy partition due to electronic mode is built in. In this approach it is assumed that the electronic temperature equilibrates with the vibrational temperature and hence the electron-electronic energy equation is not solved. Justification for adopting two-temperature model is described in detail in [14]. However, to include the electronic energy into account without solving a separate electron-electronic energy equation, the vibrational energy equation of the non-ionizing two temperature model is replaced by the vibrational-electron-electronic energy conservation equation. In this equation, the effects of energy exchanges due to electrons are taken into account in the form of source terms. Also the vibrational-electron-electronic energy consists of the species electronic energy terms described by the characteristic electronic temperature and the degeneracy of various energy levels.

The species considered in the seven species model are N_2, O_2, NO, N, O, NO^+ and e^-. The first five species are the neutral components of the air; the next two are the single component ion and free electron respectively. The governing fluid dynamic conservation equations used in the present work are the Navier–Stokes equation in the Cartesian frame and the vector form of the conservative equations are represented as

$$\frac{\partial U}{\partial t} + \nabla \cdot \left(\vec{F}^{(i)} - \vec{F}^{(v)} \right) = \vec{\Omega}_{cv} \tag{1}$$

where, the superscript i represents the inviscid terms and v represents the viscous terms. $\vec{\Omega}_{cv}$ represents the source terms of the chemical reactions and vibrational energy equations. The equation sets are defined for conservation of mass for the number of species (ns) considered along with a conservation of mass of gas mixture, three momentum conservation equations and two energy equations. The energy equations include modeling of the vibrational relaxation process and conservation of total of energy. The above description of conservation set of equations is referred to as 'The two-temperature model'. The integral forms of above equations are

$$\frac{\partial}{\partial t} \int_V U dV + \int_{A(V)} \left(\vec{F}^{(i)} - \vec{F}^{(v)} \right) dA + = \int_V \vec{\Omega}_{cv} dV \tag{2}$$

In the finite volume framework, the above equation in Cartesian form is represented by

$$\frac{d\boldsymbol{U}}{dt} V + \sum_{A(V)} \left(\vec{F}^{(i)} - \vec{F}^{(v)} \right) \cdot \hat{n} dA = \vec{\Omega}_{cv} V \tag{3}$$

where, $\boldsymbol{U}$ is the conserved variable vector, $A(V)$ is the surface enclosing the volume V. The flux vector is denoted by $\vec{F}$, $\hat{n}$ is the outward normal vector of surface $A(V)$ and $\vec{\Omega}_{cv}$ is the source term vector.

The conserved variable, inviscid, viscous fluxes and source term vectors are defined [9] as

$$\vec{U} = \begin{bmatrix} \rho_s \\ \rho \\ \rho \vec{\boldsymbol{u}} \\ \rho e \\ \rho e_{ve} \end{bmatrix}; \tag{4}$$

$$\overrightarrow{F}^{(i)} \cdot \hat{n} = \begin{bmatrix} \rho_s U_n \\ \rho U_n \\ \rho U_n \vec{\boldsymbol{u}} + p.\hat{n} \\ (\rho e + p) U_n \\ \rho e_{ve} U_n \end{bmatrix} \tag{5}$$

$$\overrightarrow{F}^{(v)} \cdot \hat{n} = \begin{bmatrix} -\boldsymbol{J_{sj}} \cdot \hat{n} \\ 0 \\ \overline{\overline{\tau}}_{ij} \cdot \hat{n} \\ \vec{\boldsymbol{u}}^{\boldsymbol{T}} \overline{\overline{\tau}} \cdot \hat{n}_j - \vec{\boldsymbol{q}} \cdot \hat{n} \\ -\boldsymbol{J_s} h_s \cdot \hat{n} - \vec{q}_{ve} \cdot \hat{n} - \boldsymbol{J_s} e_{ve} \cdot \hat{n} \end{bmatrix} \tag{6}$$

$$\overrightarrow{\Omega} = \begin{bmatrix} \omega_{c,s} \\ 0 \\ 0 \\ Q_{tr,JH} + Q_{ve,JH} \\ \omega_{ve} + Q_{ve,JH} \end{bmatrix} \tag{7}$$

Author's personal copy

In the above equations, ρ is the density of the gas mixture, and ρ_1, ρ_2 ...ρ_{ns} are the species densities, u, v, w are the Cartesian velocity components, U_n is the contravariant velocity, p is the static pressure, e is the total energy per unit mass and e_{ve} is the vibrational-electron-electronic energy per unit mass. The subscript *'ns'* corresponds to the number of species considered.

The viscous stresses are modeled using the Stokes' hypothesis given by

$$\tau_{ij} = -\mu\left(\frac{\partial u_i}{\partial x_j} + \frac{\partial u_j}{\partial x_i}\right) + \frac{2}{3}\mu\frac{\partial u_k}{\partial x_k}\delta_{ij} \tag{8}$$

where, μ is the molecular viscosity of the mixture and δ_{ij} is the Kronecker delta. The term $\vec{u}^T$ is the transpose matrix of velocity components and $\bar{\bar{\tau}}$ is the viscous stress tensor. The mass diffusive flux of each specie's' is modeled using the Fick's law of mass diffusion given by $\vec{J}_{s\neq e} = \overrightarrow{I_s} - C_s\sum_{r\neq e}\vec{I}_r$ with $\overrightarrow{I_s} = -\rho D_s \nabla C_s$ where C_s is the mass fraction of the species and D_s is the species mass diffusion coefficient. The heat flux terms which defines the thermal diffusion is modeled using Fourier's law of heat conduction given by

$$\vec{q} = -(\kappa_t + \kappa_r)\frac{\partial T_t}{\partial x_k} - \kappa_{ve}\frac{\partial T_{ve}}{\partial x_k} + \sum_{s=1}^{ns} J_s h_s \tag{9}$$

where, the total enthalpy is, $h_s = e_s + R_s T$, T is the translational temperature, T_{ve} is the vibrational temperature, κ_t and κ_r are the thermal conductivities due to the translational and rotational energy modes, κ_{ve} is the thermal conductivity due to vibrational-electron-electronic mode and R_s is the species gas constant. In the present model electron temperature is assumed to be equilibrated with the vibrational temperature. The total energy conservation equation and the vibrational energy conservation equation have been modeled with addition of Joule heat sources. The Joule heating source terms corresponding to the translational and vibrational energy modes are represented by $Q_{tr,JH}$ and $Q_{ve,JH}$ in Eq. (7). Further information on the ionization model based on two-temperature method and Park's model can be obtained from [14].

Finite-Rate Air Chemistry Model

The 7-species reaction model considered here consists of the following six reactions:

$$\begin{aligned}
R1: &\quad N_2 + \mathcal{M} \rightleftharpoons 2N + \mathcal{M}\\
R2: &\quad O_2 + \mathcal{M} \rightleftharpoons 2O + \mathcal{M}\\
R3: &\quad NO + \mathcal{M} \rightleftharpoons N + O + \mathcal{M}\\
R4: &\quad N_2 + O \rightleftharpoons NO + N\\
R5: &\quad NO + O \rightleftharpoons O_2 + N\\
R6: &\quad N + O \rightleftharpoons NO^+ + e^-
\end{aligned} \tag{10}$$

Here, $\mathcal{M}$ is the impacting body which can be any one of the five species. The reaction $R1$–$R3$ are the heavy-particle impact dissociation reactions and the forward reaction rate depends on the vibrational excitation of the molecules. The reactions $R4$ and $R5$ are exchange reactions or the Zeldovich Reactions. The reaction $R6$ is the called the dissociative recombination reaction. The Park model [12] is used for solving the chemical reactions and the forward reaction rate coefficients are obtained using the Arrhenius equation, with the backward reaction rate coefficient obtained using the forward rate coefficient and the equilibrium constant. Park's air chemistry model uses an effective temperature that blends the translational-rotational temperature and the vibrational temperature by a geometric average temperature which will be used according to the type of reaction considered.

The source terms of the vibrational-electron-electronic energy conservation equation, models the energy relaxation taking place due to energy transfer between heavy particles and electrons, work done on electrons by electron pressure gradients and production and destruction of vibrational energy which is modeled as harmonic oscillators. The translation-rotational and vibrational energy exchange is modeled using the Landau-Teller equation. More details on the finite rate air-chemistry model can be referred from [14].

Hypersonic Flow Control Actuation Using Plasma Discharge

Adopting the plasma discharge for control actuation in hypersonic flow regime is a non-intrusive technique, which shall be regarded as an advanced futuristic and innovative approach when compared to the intrusive means. Though wind tunnel experiments involving hypersonic flow with plasma discharge for actuation studies are gaining importance, not many numerical simulation codes are available for mimicking the complex physics associated with the problem. The flow field complexity stems from the fact that, due to the interaction of cold hypersonic stream with the ionized plasma in the discharge zone, the energy partition due to vibrational mode gets excited in spite of the translational-rotational mode being dormant. Hence to mimic the complex flow interactions, it is necessary to model all the relevant physics of flow such as the multi-species air-chemistry involving vibrational excitation, ionization and the appropriate models for simulating the plasma discharge.

A novel flow actuation technique has been adopted in modeling ionizing hypersonic flow field involving plasma discharge, by considering all the relevant mathematical models, adopting them within the framework of CERANS-

Author's personal copy

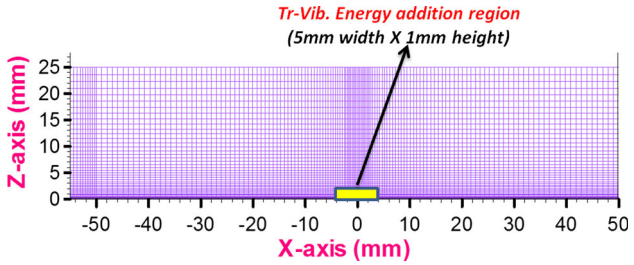

Fig. 1 Computational domain and grid

TCNEQ solver, and demonstrated through an application of control actuation in a hypersonic flow presented in the following sections.

Simulation Details

Figure 1 shows the computational setup for the present numerical simulation depicting the location and size of plasma discharge region. The grid consists of 151 × 4 ×71 points amounting to about 40,000 cells. Since the problem is two dimensional, and the CERANS-TCNEQ code is three dimensional, three cells in the span-wise direction with symmetric boundary conditions have been used for modeling 2D flow. The length of flat plate is about 100 mm (x-location varies from −50 mm to +50 mm) and the discharge region with a length of 5 mm and height of 1 mm is located at 50 mm from the leading edge of the plate. The flow is considered laminar and the wall temperature had been fixed at 300 K. The values of energy addition represented as consumed energy in the experiments of Watanabe and Suzuki [8] was about 100 W per 2 cm width which implies that the plasma energy generated and discharged by the electrodes is about 5 kW/m. In their numerical experiments [8], the translational and vibrational energy addition was set to be 40 % of the consumed energy, so that the resulting pressure change as well as the two temperatures corroborates with the experimental results. Therefore, the total Joule heating source is about 2 kW/m partitioned into 1 kW/m each for the translational and vibrational energy modes and is deposited

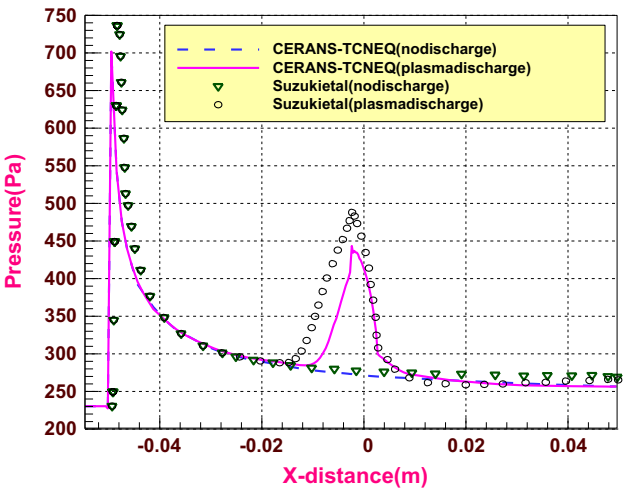

Fig. 3 Comparison of surface pressure distribution

uniformly in the region marked in Fig. 1 and held constant throughout the flow evolution.

Let the heat addition of the experiment in the Joule heating region represented by S be $Q_{exp} = 100$ W per 2 cm, equivalent to a net input energy per unit depth of 5 kW/m, then the expression for $Q_{tr,JH}$ and $Q_{ve,JH}$ are given by

$$Q_{i,JH}(x,y) = \begin{cases} q_i & (if(x,y) \in S) \\ 0 & (if(x,y) \notin S) \end{cases} \quad i = tr, ve \tag{11}$$

where $\int_S q_i dS = Q_{exp} \times 0.40$

Results and Discussions

The pressure contours of the simulation with heat addition are shown in Fig. 2. The leading edge shock can be clearly observed with a rapid flow recovery downstream till it reaches the plasma discharge zone. Due to the heat addition in the plasma discharge zone, a shock wave is created and locally an increase in pressure is observed. The pressure distribution on the flat plate with and without plasma discharge is shown in Fig. 3 along with comparison of data

Fig. 2 Pressure contours (Pa)

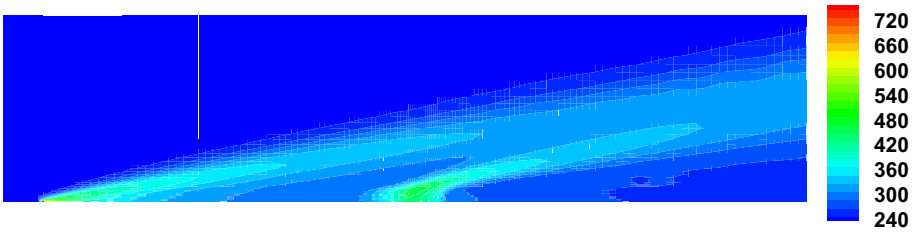

Author's personal copy

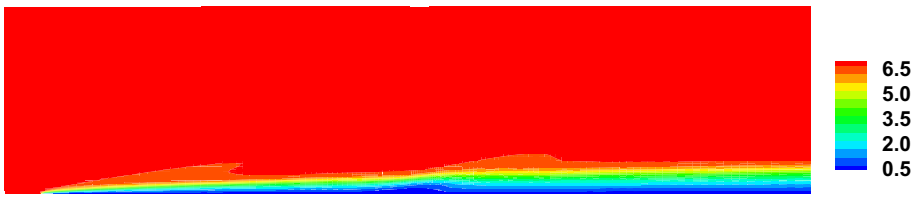

Fig. 4 Mach contours

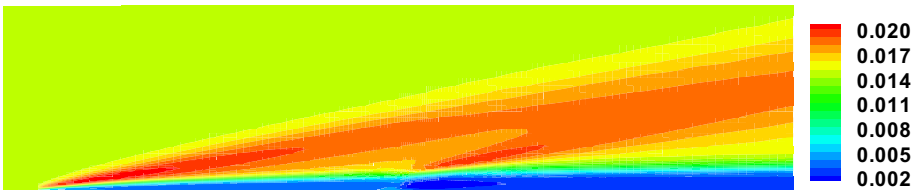

Fig. 5 Density contours

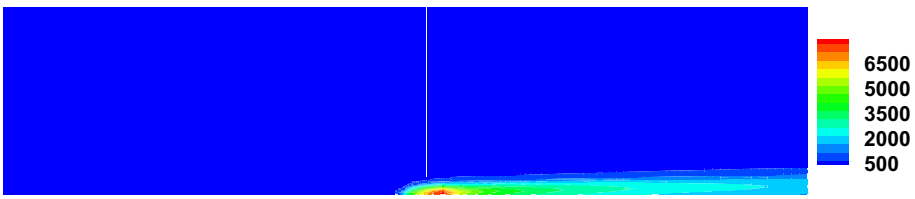

Fig. 6 Vibrational temperature contours

from [8]. It shows the pressure rise due to leading edge shock from the freestream value of 230 Pa to about 700 Pa for both the cases. For the flow without plasma discharge the downstream pressure recovery towards the freestream pressure is rapid and continuous. In case of the plasma discharge, downstream of the leading edge shock, the surface pressure rapidly decreases to about 300 Pa at x location of -10 mm similar to the no-discharge case before encountering the plasma discharge region.

Due to disturbance created by the plasma discharge region which is similar to the flow disturbance caused by a physically protruding component, a shock wave is formed ahead of the discharge region and it is depicted by a discontinuous pressure rise in the region between -10 mm and about -3 mm to a value of about 450 Pa. Also, the upstream cold flow is not able to penetrate the thermal region created due to the plasma discharge. This is due to the fact that the plasma discharge area acts similar to a solid obstacle and the cold flow circumvents the region with only a little amount of flow going through the plasma region. Further downstream, surface pressure decreases discontinuously from about -3 mm to about 4 mm before reaching a plateau of about 270 Pa. The pressure

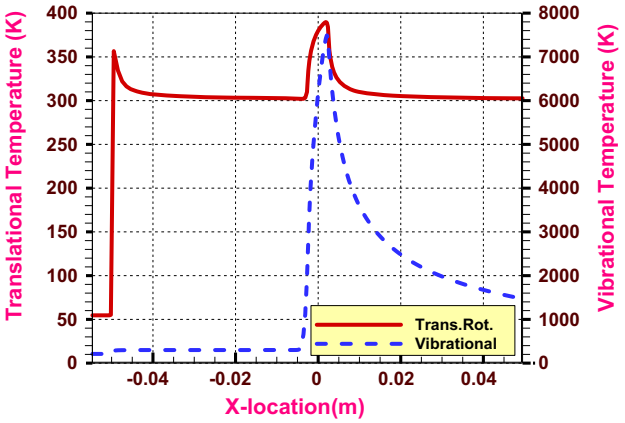

Fig. 7 Surface temperature distribution

distribution due to Watanabe and Suzuki [8] shows a slightly larger pressure rise around the plasma discharge zone when compared to the present simulation data. The pressure discontinuity due to plasmas discharge starts at about 14 mm and the peak value of about 490 Pa had been observed at about -3 mm. The difference in results can be attributed mainly to the number of species modeled in the

Author's personal copy

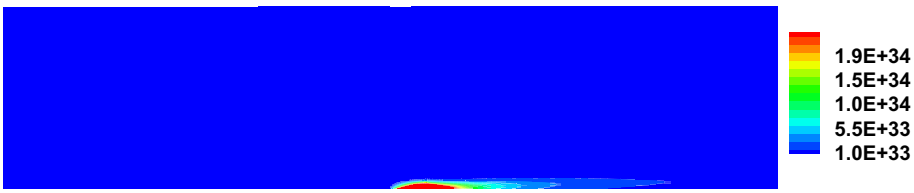

Fig. 8 Contours of $n_{N2}T_v^4$ depicting the glow due to plasma discharge

air-chemistry which is 7 in case of the present simulation and 11 in case of [8]. Qualitatively, the agreement between two results can be observed to be good. Further downstream of the plasma discharge zone, the results of present prediction and that of [8] are almost identical.

The Mach number contours are shown in Fig. 4. The growth of boundary layer from the leading edge of the plate can be clearly observed. However it is interesting to note that the boundary layer is only slightly disturbed by the plasma discharge. The density contours depicted in Fig. 5 shows low dense region near the wall due to the isothermal wall temperature of 300 K. However due to the shock at the leading edge and the plasma discharge region, an increase in flow density can be observed.

The vibrational temperature contours are shown in Fig. 6. It can be observed that the vibrational excitation caused due to heat addition in its energy partition increases the vibrational temperature locally to about 7000 K followed by a hotter wake downstream of the discharge region. The surface distributions of translational-rotational and vibrational temperatures are presented in Fig. 7. It can be observed that the translational rotational temperature had reached a peak value of about 360 K at the leading edge and reaches the imposed isothermal wall temperature immediately downstream. Since such low translational temperature is inadequate for vibrational excitation of the molecular species of the air, there is no variation of vibrational temperature in this region. In the plasma discharge zone, the translational temperature increases marginally and reaches a peak value of about 390 K. Due to plasma discharge, the vibrational excitation takes place, however without any molecular dissociation and the vibrational temperature reached a peak value of about 7500 K. Similar observation had been found in [8] also.

Watanabe and Suzuki [8] have presented the contours of glow due to plasma discharge as vibrational excitation of nitrogen molecule. It can be represented by Stefan-Boltzmann equation as $n_{N2}T_v^4$, where n_{N2} is the number density of the N_2 species and T_v is the vibrational temperature. The contours of $n_{N2}T_v^4$ are presented in Fig. 8 which clearly shows the concentration of glow region around the plasma discharge. These results corroborate well with the results of [8].

Conclusion

A novel method has been developed for computational modeling of the ionizing hypersonic flow with plasma discharge by considering relevant mathematical models for multispecies air-chemistry interactions, vibrational relaxation, ionization and Joule heating source terms, within the CERANS-TCNEQ framework and demonstrated for a proof-of-concept hypersonic flow-control problem.

Hypersonic flow over a flat plate subjected to surface plasma discharge had been studied. The glow occurring due to the plasma discharge had been mimicked in the computational model similar to that of the experiment. Due to the plasma discharge, the surface pressure had increased by about 30 %. This phenomenal increment in pressure can be used to the advantage for maneuvering and steering hypersonic flight vehicles. This proof of concept study has clearly demonstrated the capability of CERANS-TCNEQ in modeling the complex non-equilibrium hypersonic flow with Joule heating sources for flow control.

Acknowledgment This paper is a revised version of an article entitled ''Numerical Simulation of Non-Equilibrium Plasma Discharge for Flow Control of Aerospace Vehicles'' presented at the Twenty-eighth National Convention of Aerospace Engineers held at Bangalore during November 14–15, 2014 organized by The Institution of Engineers (India), Karnataka State Centre.

References

1. A.L. Kuranov, E.G. Sheikin, MHD control by external and internal flows in Scramjet under "AJAX" Concept", AIAA-2003-173, in *41st Aerospace Sciences Meeting and Exhibit*, Reno, Neveda, USA, Jan 2003
2. Y. Watanabe, K.Suzuki, Effect of impulsive plasma discharge in hypersonic boundary layer over flat plate, AIAA-2011-3736, in 42nd *AIAA Plasmadynamics and Lasers Conference*, Honolulu, Hawaii, USA, June 2011
3. R. Balasubramanian, K. Anandhanarayanan, R. Krishnamurthy, D. Chakraborty, Hypersonic aerothermodynamics simulation toolkit, 16th Annual CFD *Symposium of Aeronautical Society of India*, Bengaluru, India, Aug 2014
4. R. Balasubramanian, K. Anandhanarayanan, Development of a thermo-chemical non-equilibrium solver for hypervelocity flows. J. Inst. Eng. (India): Ser.-C, IEI-C, doi:10.1007/s40032-014-0166-5. (Published online: 25 Dec 2014)
5. R. Balasubramanian, K. Anandhanarayanan, Development of a thermo-chemical non–equilibrium solver for weakly Ionized

Author's personal copy

hypersonic flowfields. J. Aerosp. Sci. Technol. **67**(1), 45–67 (2015)
6. L. Yang, Flow control using energy deposition at Mach 5, Ph.D. thesis, School of Mechanical, Aerospace and Civil Engineering, University of Manchester, 2012
7. J.S. Shang, S.T. Surzhikov, R. Kimmel, D. Gaitonde, J. Menart, J. Hayes, Plasma actuators for hypersonic flow control, AIAA 2005-0562, in *43rd AIAA Aerospace Sciences Meeting and Exhibit, Reno*, Neveda, USA, Jan 2005
8. Y. Watanabe, K. Suzuki, Study of nonequilibrium plasma discharge in hypersonic flow over flat plate, AIAA 2013-0460, in *51st AIAA Aerospace Sciences Meeting, Grapevine,* Texas, USA, Jan 2013
9. Y. Watanabe, K. Suzuki, Investigation of arc plasma discharge in Hypersonic flow over compression and expansion corner, AIAA 2013-3130, in *44th AIAA Plasmadynamics and Lasers Conference*, San Diego, CA, USA, June 2013
10. R. Balasubramanian, K. Anandhanarayanan, Higher order accurate reconstruction scheme for the Navier-Stokes equations on finite volume polyhedral grids, in *Proceedings of the Seventh Asian Computational Fluid Dynamics Conference, ACFD-7*, Bangalore, India, pp. 875–883, 26–30 Nov 2007
11. R. Balasubramanian, J. Prabhu Dayal, R. Krishnamurthy, Debasis Chakraborty, Aero-propulsive characterization of an airborne vehicle with two side-jets using CERANS, in *Proceedings of the 6th Symposium on Applied Aerodynamics and Design of Aerospace Vehicles (SAROD 2013),* Hyderabad, India, 21–13 Nov 2013
12. C. Park, *Nonequilibrium Hypersonic Aerodynamics* (Wiley, NewYork, 1990)
13. P.A. Gnoffo, R.N. Gupta, J.L. Shinn, Conservation equations and physical models for hypersonic air flows in thermal and chemical nonequilibrium, in *NASA Technical Paper 2867*, Feb 1989
14. L.C. Scalabrin, Numerical simulation of weakly ionized hypersonic flow over reentry capsules, Ph.D. thesis, Aerospace Engineering, University of Michigan, USA, 2007